Preparation of Amphiphilic Copolymers for Covalent Loading of Paclitaxel for Drug Delivery System

Wulian Chen,[1] Jin Z. Zhang,[2] Jianhua Hu,[1,3] Qisang Guo,[4] Dong Yang[1]

[1]State Key Laboratory of Molecular Engineering of Polymers, Department of Macromolecular Science, Fudan University, Shanghai 200433, China
[2]Department of Chemistry and Biochemistry, University of California, Santa Cruz, California 95064
[3]Key Laboratory of Smart Drug Delivery, Ministry of Education and PLA, Fudan University, Shanghai 201203, China
[4]Mdical Center for Diagnostics & Treat of Cervical Disease, Obstetrics and Gynecology Hospital, Fudan University, Shanghai 200011, China
Correspondence to: J. Hu (E-mail: hujh@fudan.edu.cn) or D. Yang (E-mail: yangdong@fudan.edu.cn)

Received 14 July 2013; accepted 31 October 2013; published online 18 November 2013
DOI: 10.1002/pola.27009

ABSTRACT: A novel drug-polymer conjugate was prepared by the copper-catalyzed azide–alkyne cycloaddition reaction between an azide-functional diblock copolymer and an alkyne-functional paclitaxel (PTX). The well-defined azide-functional diblock copolymer, poly(ethylene glycol) (PEG)-*b*-P(OEGEEMA-*co*-AzPMA), was synthesized via the atom transfer radical polymerization of oligo(ethylene glycol) ethyl ether methacrylate (OEGEEMA) and 3-azidopropyl methacrylate (AzPMA), using PEG-Br as macroinitiator and CuBr/PMDETA as a catalytic system. The alkyne-functional PTX was covalently linked to the copolymer via a click reaction, and the loading content of PTX could be easily tuned by varying the feeding ratio. Transmission electron microscopy and dynamic light scattering results indicated that the drug loaded copolymers could self-assemble into micelles in aqueous solution. Moreover, the drug release behavior of PEG-*b*-P(OEGEEMA-*co*-AzPMA-PTX) was pH dependent, and the cumulative release amount of PTX were 50.0% at pH 5.5, which is about two times higher than that at pH 7.4. The *in vitro* cytotoxicity experimental results showed that the diblock copolymer was biocompatible, with no obvious cytotoxicity, whereas the PTX-polymer conjugate could efficiently deliver PTX into HeLa and SKOV-3 cells, leading to excellent antitumor activity. © 2013 Wiley Periodicals, Inc. J. Polym. Sci., Part A: Polym. Chem. **2014**, *52*, 366–374

KEYWORDS: amphiphilic copolymer; atom transfer radical polymerization; click reaction; covalent loading; diblock copolymers; drug delivery system; micelles; prodrug

INTRODUCTION Chemotherapy is one of the most widely used strategies in the long history of combating cancer.[1,2] However, most of the anti-cancer drugs, that is, paclitaxel (PTX) and doxorubicin (DOX), often suffer from intrinsic limitations, such as poor water-solubility, severe side effects, and low therapeutic index.[3–10] To solve these problems, various drug delivery systems (DDSs) have been developed and investigated in the past decades.[11–19]

Amphiphilic copolymers are frequently used as drug carriers in DDSs. In aqueous solution, amphiphilic copolymers could self-assemble to form micelles, which are composed of two distinct domains, a hydrophobic core and a hydrophilic shell. Thus, hydrophobic drugs could be entrapped into the core,[20] and the hydrophilic shell, in general poly(ethylene glycol) (PEG), could effectively protect the core against the external biological media, inhibit nonspecific protein absorption, and increase the plasma clearance half-life.[21,22] Furthermore, the size of the polymeric micelle is about several dozens of nanometers, which affords the polymeric micelles passive targeting function to tumor tissues via the enhanced permeability and retention (EPR) effect.[23,24]

Up to date, most of the DDSs using polymeric micelles as drug carriers load drugs via noncovalent interactions.[25–30] For example, Lee et al. have prepared an amphiphilic block copolymer, poly(ethylene glycol)-*b*-poly(2-(4-(vinylbenzyloxy)-*N,N*-diethylnicotinamide)) (PEG-*b*-P(VBODENA)), that could form a core-shell micelle in aqueous solution.[31] PTX was then incorporated in the polymeric micelles via physical entrapment. However, to these DDSs, many factors, such as high dilution, pH, temperature, ionic strength, large shear forces during blood circulation, and the presence of numerous charged blood components, can affect their stability.[32,33] This could lead to burst release of drug,[34–37] which is the main reason for toxic and side effects and dramatically

Additional Supporting Information may be found in the online version of this article.

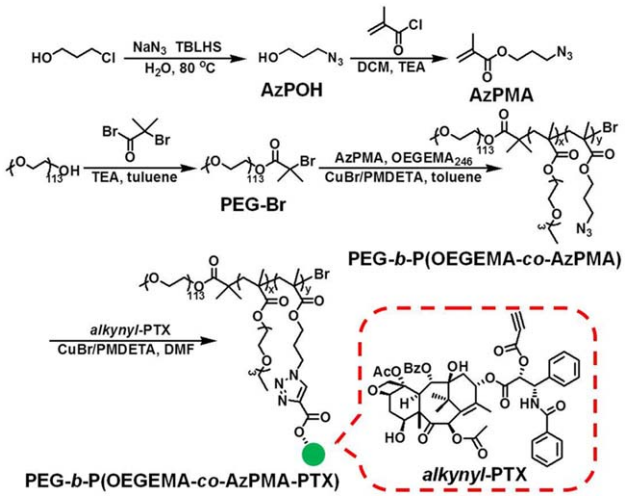

SCHEME 1 Synthetic routes used for the preparation of alkynyl-PTX, PEG-b-P(OEGEEMA-co-AzPMA) diblock copolymer and PEG-b-P(OEGEEMA-co-AzPMA-PTX) prodrug. [Color figure can be viewed in the online issue, which is available at wileyonlinelibrary.com.]

decreases the therapeutic efficacy. Thus, an alternative DDS based on polymer with covalent loading of drug, polymeric micellar drug conjugate, has been proposed to overcome the problems mentioned above. As compared to polymeric micelle DDSs loading drug via physical entrapment, polymeric micellar drug conjugate DDSs are more stable and typically have continuous release without burst release effect.[38–41] Commonly, the drug and the polymer was conjugated via relatively stable linkers (e.g. amide and ester bonds). For example, Kwon et al. have covalently linked PTX to poly(ethylene glycol)-block-poly(aspartate-hydrazide-levulinic acid) (PEG-p(Asp-HydLEV)) through ester bonds and found that PTX could continuously low dose release.[42,43] Due to the only reactive functional hydroxyl group in PTX, the existing strategies to synthesize PTX-polymer conjugates are difficult and tedious. Therefore, it is of strong interest to explore a facile and efficient way to construct PTX-polymer conjugates.

The recent development of click chemistry provided a powerful tool for synthetic polymer chemistry and the pharmaceutical fields.[44–47] Due to its high efficiency and selectivity, moderate reaction condition and simple purification, the azide–alkyne reaction has been widely used to prepare drug-polymer conjugates. Herein, we constructed a novel PTX-polymer conjugate based on copolymer covalently linked to PTX via an azide–alkyne reaction (Scheme 1). Well-defined azide-functional diblock copolymer, PEG-*b*-P(OEGEEMA-*co*-AzPMA), was synthesized via atom transfer radical polymerization (ATRP) of oligo(ethylene glycol) ethyl ether methacrylate (OEGEEMA) and 3-azidopropyl methacrylate (AzPMA). Then, alkyne-functional PTX was covalently linked to the copolymer via an azide–alkyne reaction. The chemical structures of the diblock copolymer and PTX-polymer conjugate were characterized by proton-nuclear magnetic resonance (^{1}H NMR), gel permeation chromatography (GPC), Fourier transformed infrared (FT-IR), ultraviolet (UV) spectra, and so on. The *in vitro* cellular cytotoxicity experiments were performed to evaluate the biocompatibility of the copolymer, and the anticancer activity of the PTX-polymer conjugate to HeLa and SKOV-3 cells.

EXPERIMENTAL

Materials

Paclitaxel (PTX) was purchased from Beijing Huafeng United Technology Co., Ltd. Oligo(ethylene glycol) ethyl ether methacrylate (OEGEEMA, $M_n = 246$ g mol^{-1}, 99%) purchased from Aldrich was passed through a neutral alumina column to remove the inhibitor prior to use. Triethylamine (TEA, 99.5%, Aldrich) was dried over CaH_2 and distilled at 110 °C. Toluene (Aldrich, 99%) was refluxed with sodium beads/benzophenone complex and distilled until the solution turned purple. Copper(I) bromide (CuBr, 99.999%, Aldrich), *N,N,N′,N″,N*[tprime]-pentamethyldiethylenetriamine (PMDETA, 98%, Aldrich), 2-bromoisobutyl bromide (B*i*BB, 98%, Acros), 3-chloropropanol (99.5%, J&K CHEMICA), and sodium azide (NaN_3, 98%, SCR) were used as received without further purification.

Synthesis of Alkynyl-Paclitaxel

Alkyne-PTX was synthesized by the esterification of PTX with propiolic acid. In a typical procedure, palitaxel (420 mg, 0.49 mmol), propiolic acid (0.3 mL, 4.9 mmol), 4-dimethylamiopyridine (DMAP) (10 mg), *N,N*'-diisopropylcarbodiimide (DIC) (0.1 mL), and CH_2Cl_2 (20 mL) were added into a 100-mL of flask. The mixture was stirred at room temperature for 6 h. A yellowish solid (0.38 g, yield of 83.2%), alkyne-PTX, was obtained by passing through silica column chromatography (eluent: diethyl ether/hexane/ethyl acetate (v:v) = 1/1/1), and evaporating.

Block Copolymerization of AzPMA and OEGEEMA

PEG-Br macroinitiator was prepared by the esterification of PEG-OH with 2-bromoisobutyl bromide according to refs. 48–50, and 3-azidopropyl methacrylate (AzPMA) were synthesized according to ref. 51 (See Supporting Information). PEG-*b*-P(OEGEEMA-*co*-AzPMA) block copolymer was obtained by ATRP of AzPMA and OEGEEMA using PEG-Br as macroinitiator and CuBr/PMDETA as a catalytic system.[52–57] In a typical procedure, a dry 50 mL Schlenk flask (flame-dried under vacuum prior to use) was charged with PEG-Br (2.0 g, 0.39 mmol) and CuBr (57.2 mg, 0.4 mmol). Then, AzPMA (0.95 mL, 6.0 mmol), OEGEEMA (2.0 mL, 10.0 mmol), dry toluene (10 mL), and PMDETA (0.16 mL, 0.8 mmol) was introduced via a gas-tight syringe. The mixture was degrassed with three freeze-evacuate-thaw cycles followed by immersing into an oil bath at 80 °C. The polymerization lasted 6 h and was terminated by immersing the flask into liquid N_2. The mixture was diluted with THF and passed through a short neutral alumina column to remove the residual copper catalyst. The solution was concentrated under vacuum and precipitated into cold hexane. After repeated purification

by dissolving in THF and precipitating in cold hexane, a waxy solid, PEG-*b*-P(OEGEEMA-*co*-AzPMA), was obtained by drying *in vacuo* overnight.

GPC: $M_n = 14{,}000$ g mol^{-1}, $M_w/M_n = 1.29$. ^{1}H NMR ($CDCl_3$): 0.77–0.95 (3H, CH_3CCH_2 of POEGMEA and PAzPMA), 1.22 (3H, CH_3CH_2O of POEGMEA), 1.85 (2H, CH_2CCH_3 of POEGMEA and PAzPMA), 1.92 (2H, $CH_2CH_2N_3$), 3.37 (3H, CH_3O of PEG), 3.44 (2H, $CH_2CH_2N_3$), 3.64 (4H, OCH_2CH_2 of PEG and POEGMEA), 4.0–4.1 (2H, $COOCH_2$ of POEGMEA and PAzPMA). FT-IR: 2100 cm^{-1} (ν_{N_3}).

Synthesis of Drug-polymer Conjugate PEG-b-P(OEGEEMA-co-AzPMA-PTX)

Drug-polymer conjugate, PEG-*b*-P(OEGEEMA-*co*-AzPMA-PTX), was synthesized by copper(I)-mediated azide–alkyne click reaction of PEG-*b*-P(OEGEEMA-*co*-AzPMA) with alkyne-PTX. Briefly, to a 10-mL of flask, alkyne-PTX (0.09 g, 0.10 mmol of alkyne groups), PEG-*b*-P(OEGEEMA-*co*-AzPMA) (0.12 g, 0.10 mmol of N_3 groups), and PMDETA (0.16 mL, 0.8 mmol) were added and dissolved with 2 mL of DMF. The mixture was degrassed with three freeze-evacuate-thaw cycles followed by the addition of CuBr (57.2 mg, 0.40 mmol). The reaction mixture was stirred for 24 h at room temperature under N_2 atmosphere. Then the mixture was diluted with CH_2CCl_2 and washed with 10 wt% aqueous EDTA and deionized water. The organic phase was dried with sodium sulfate and then precipitated into excess diethyl ether. After repeated purification by dissolving in CH_2CCl_2 and precipitating in diethyl ether, a yellowish solid, PEG-*b*-P(OEGEEMA-*co*-AzPMA-PTX), was obtained by drying *in vacuo* overnight.

In Vitro *Drug Release*

The drug release of PTX from PTX-polymer conjugate, PEG-*b*-P(OEGEEMA-*co*-AzPMA-PTX), was studied at 37 °C in two different medias, (a) PBS of pH = 5.5 and (b) PBS of pH = 7.4. Typically, 5 mg of PTX-polymer conjugate was dissolved in 5 mL of deionized water. 2 mL of solution was transferred to a dialysis bag with an molecular weight cut-off (MWCO) of 3500 and then immersed in 250 mL of pH = 5.5 or pH = 7.4 PBS at 37 °C with constant shake. Periodically, 20 mL of external buffer solution was removed and replaced with equal volume of fresh medium. Upon each sampling, 20 mL of PBS was lyophilized and then dissolved in acetonitrile and PTX concentration was quantified by measuring the absorbance at 229 nm against a standard curve.

In Vitro *Cell Assay*

The cytotoxicity of PEG-*b*-P(OEGEEMA-*co*-AzPMA) was evaluated in HeLa, SKOV-3 and HEK-293 cells by CCK-8 kit asssys. The cells were seeded in 96-well plates with a density of 1×10^4 cell per well and incubated at 37 °C in an atmosphere containing 5% CO_2 for 24 h to allow cell attachment. Then, the medium was replaced with a fresh medium containing the indicated concentration of PEG-*b*-P(OEGEEMA-*co*-AzPMA). After incubation for 24 and 48 h, the medium was aspirated and replaced by 100 μL of fresh medium containing 10 μL of CCK-8. The cells were incubation for another 2 h at 37 °C in dark. Afterward, the absorbance at a wavelenth of 450 nm of each well was measured using a microplate reader. The relative cell viability (in percentage) was determined by the following equation:

$$\text{Cell viability } (\%) = \frac{I_{\text{sample}} - I_{\text{blank}}}{I_{\text{control}} - I_{\text{blank}}}$$

where I_{sample}, I_{control}, and I_{blank} represent the absorbance intensity at 450 nm determined for cells teated with different samples, for control cells (nontreated), for blank well without cells, respectively.

The antitumor activity of PEG-*b*-P(OEGEEMA-*co*-AzPMA-PTX) was studied in a similar way. Briefly, HeLa and SKOV-3 cells were seeded in 96-well plates with a density of 1×10^4 cell per well and incubated at 37 °C in an atmosphere containing 5% CO_2 for 24 h to allow cell attachment. Then, the medium was replaced with a fresh medium containing the indicated concentration of PEG-*b*-P(OEGEEMA-*co*-AzPMA-PTX) for 24 and 48 h. The following procedure of the cell viability determined by CCK-8 assays was same as described above.

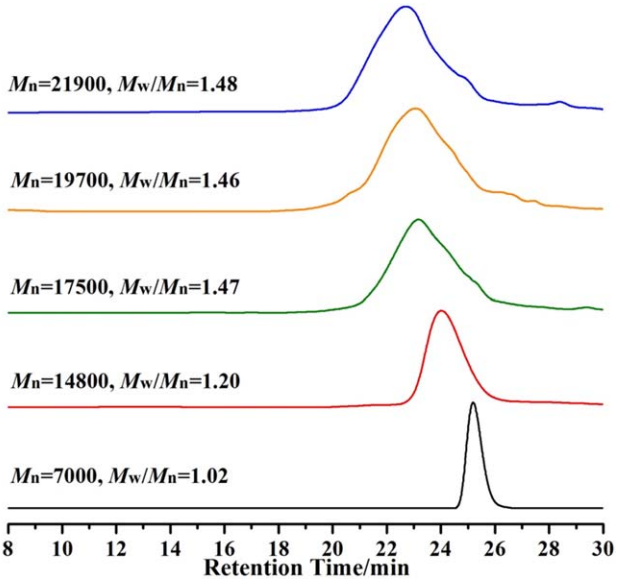

FIGURE 1 GPC traces for (A) PEG-Br, (B) PEG-*b*-P(OEGEEMA-*co*-AzPMA), (C) PEG-*b*-P(OEGEEMA-*co*-AzPMA-PTX)$_1$, (D) PEG-*b*-P(OEGEEMA-*co*-AzPMA-PTX)$_2$, and (E) PEG-*b*-P(OEGEEMA-*co*-AzPMA-PTX)$_3$ with THF as the elute. [Color figure can be viewed in the online issue, which is available at wileyonlinelibrary.com.]

Characterization

^{1}H NMR spectra were recorded on a Bruker Avance 500 spectrometer using $CDCl_3$ as solvent, trimethylsilane was used as internal standard. FT-IR measurements were performed on a NEXUX-470 spectrometer. The molecular weight and molecular weight distribution were determined by GPC. The GPC was performed in THF at 35 °C with an elution rate of 1.0 mL min^{-1} on Aginent 1100 equipped with a G1310A pump, a G1362A refractive index detector, and a G1314A

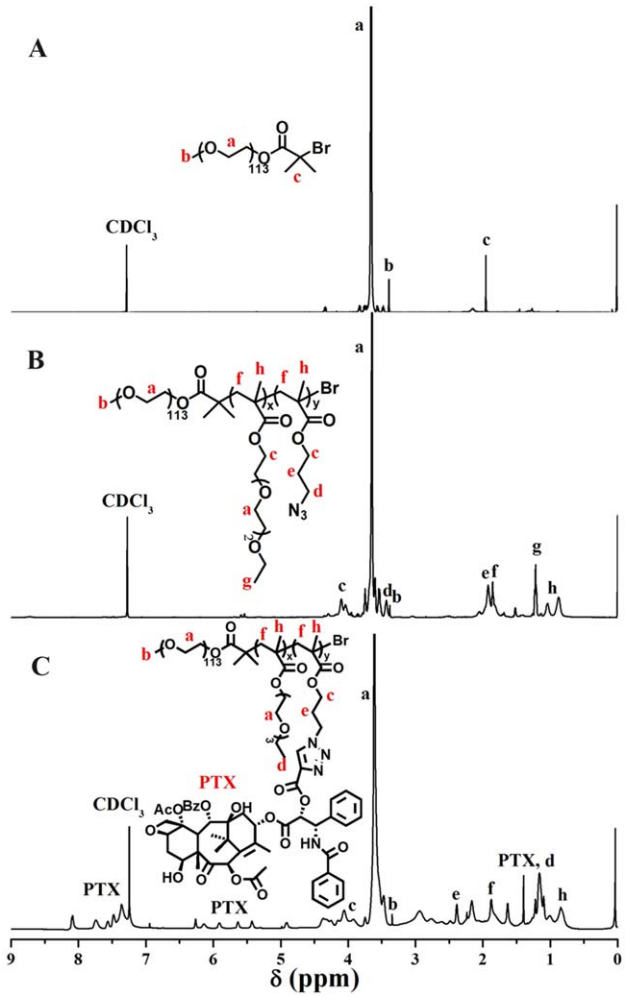

FIGURE 2 ^{1}H NMR spectra of (A) PEG-Br, (B) PEG-*b*-P(OEGEEMA-*co*-AzPMA), and (C) PEG-*b*-P(OEGEEMA-*co*-AzPMA-PTX)$_3$ in $CDCl_3$. [Color figure can be viewed in the online issue, which is available at wileyonlinelibrary.com.]

variable wavelength detector. Polystyrene standard samples were used for the GPC calibration. Transmission electron microscopy (TEM) images were obtained on a JEOL JEM 2100 F transmission electron microscope, and samples for TEM measurements were prepared by casting one drop of sample aqueous solution on carbon copper grids. The size distribution of the micelles was measured by dynamic light scattering (DLS) using a Malvern autosizer 4700 instrument. UV-visible (Vis) absorbance spectra were measured with a Perkin-Elmer Lambda 35 spectrophotometer.

RESULTS AND DISCUSSION

The diblock copolymer, PEG-*b*-P(OEGEEMA-*co*-AzPMA) was obtained via ATRP of OEGEEMA and AzPMA using PEG-Br as macroinitiator and CuBr/PMDETA as a catalytic system in toluene at 80 °C, as it was shown in Scheme 1. A typical GPC trace of PEG-*b*-P(OEGEEMA-*co*-AzPMA) was shown in Figure 1, it appeared a monomodal elution peak and a clear shift to

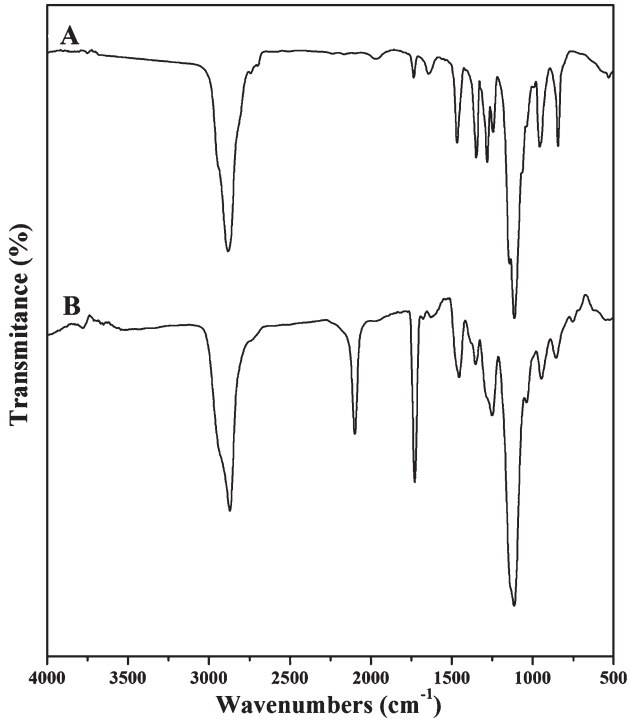

FIGURE 3 FT-IR spectra of (A) PEG-Br and (B) PEG-*b*-P(OEGEEMA-*co*-AzPMA).

the higher molecular weight side, compared with that of PEG-Br macroinitiator. The chemical structure of PEG-*b*-P(OEGEEMA-*co*-AzPMA) diblock copolymer was characterized by ^{1}H NMR. As shown in the ^{1}H NMR spectra of Figure 2(B), characteristic signals of PEG, OEGEEMA, and AzPMA were all present. The DP of P(OEGEEMA-*co*-AzPMA) was determined to be 30 with the OEGEEMA molar fraction being 0.67, as indicated in ^{1}H NMR analysis from the signal integration ratio of peaks *g* at 1.2 ppm (methyl protons at the terminal of OEGEEMA units) and *d* at 3.4 ppm (methylene protons at the α position to the azide group) relative to peak *b* at 3.3 ppm (methyl protons at the terminal of PEG). The polymer was denoted PEG-*b*-P(OEGEEMA$_{0.67}$-*co*-AzPMA$_{0.33}$)$_{30}$ and had a $M_{n,NMR}$ of 11.6 kDa, shortened as PEG-*b*-P(OEGEEMA-*co*-AzPMA) in subsequent section. Moreover, FT-IR spectrum of PEG-*b*-P(OEGEEMA-*co*-AzPMA) in Figure 3 also showed a peak at 2100 cm^{-1} characteristic for the azide vibration, and the intensity of ester bond at 1725 cm^{-1} also greatly increased after polymerization.

The PEG-*b*-P(OEGEEMA-*co*-AzPMA-PTX) drug-polymer conjugate was prepared by copper(I)-mediated azide–alkyne click reaction of PEG-*b*-P(OEGEEMA-*co*-AzPMA) with alkynyl-PTX using PMDETA as ligand in DMF at room temperature for 24 h. The drug loading content of the resulting PEG-*b*-P(OEGEEMA-*co*-AzPMA-PTX) drug-polymer conjugate could be simply tuned by varying the ratio of alkynyl group and azide group. Three different drug loading contents of PTX-polymer conjugate were obtained by three different molar ratios of alkynyl group and azide group (alkynyl:azide = 1:2, 1:1, 2:1). The reaction progress was monitored by FT-IR (by

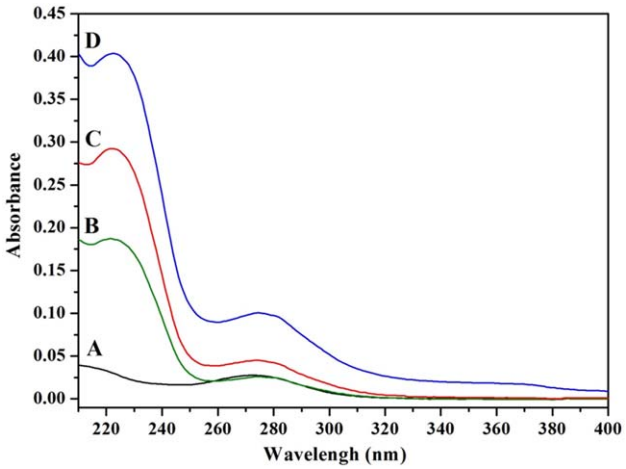

FIGURE 4 UV-Vis absorption spectra of (A) PEG-*b*-P(OEGEEMA-*co*-AzPMA) at the concentration of 100 μg mL^{-1}, (B) PEG-*b*-P(OEGEEMA-*co*-AzPMA-PTX)$_1$, (C) PEG-*b*-P(OEGEEMA-*co*-AzPMA-PTX)$_2$, and (D) PEG-*b*-P(OEGEEMA-*co*-AzPMA- PTX)$_3$ at 40 μg mL^{-1} with different PTX content. [Color figure can be viewed in the online issue, which is available at wileyonlinelibrary.com.]

the decrease of the azide vibration at 2100 cm^{-1}; Supporting Information Fig. S3). When 1:2 of alkynyl to azide ratio was used, FT-IR analysis showed that the azide peak did not disappear completely, as expected from the excess of azide used. With the increasing ratio of alkynyl to azide, the azide peak decreased and finally completely disappeared, which indicated that more alkynyl-PTX was covalently linked to

TABLE 1 Drug Loading Contents of PEG-*b*-P(OEGEEMA-*co*-AzPMA-PTX)$_s$ Determined by Differents Methods

Samples	Feed ratio of alkynyl to azide	Drug loading content (wt %) determined by		
		GPC	^{1}H NMR	UV-Vis
PEG-b-P(OEGEEMA-co-AzPMA-PTX)$_1$	1:2	14.5	12.7	12.9
PEG-b-P(OEGEEMA-co-AzPMA-PTX)$_2$	1:1	23.4	24.5	20.6
PEG-b-P(OEGEEMA-co-AzPMA-PTX)$_3$	2:1	30.5	33.2	28.5

diblock copolymer. Furthermore, the peaks near 710 cm^{-1} were also obviously increased, which were related to the C–H bending vibrations of the benzene rings in PTX. The PTX-polymer conjugate was also analyzed by GPC (Fig. 1). With the increase in PTX content, the elution peaks showed a clear shift to a higher molecular weight side. The chemical structure of PEG-*b*-P(OEGEEMA-*co*-AzPMA-PTX) diblock copolymer was characterized by ^{1}H NMR. As it could be seen from Figure 2(C), the aromatic signals at 7.0 to 8.1 ppm from PTX appeared. The characteristic signals of protons, including the 3′-CH and 5-CH protons from PTX at 5.9 and 4.9 ppm, were also observed, indicating that alkynyl-PTX was successfully covalently linked to diblock copolymer. The signal integration of the 5-CH protons from PTX at 4.9 ppm was selected to compared with that of methyl protons at the terminal of PEG at 3.4 ppm, and thus the average number of PTX in backbone could be determined. The UV-Vis

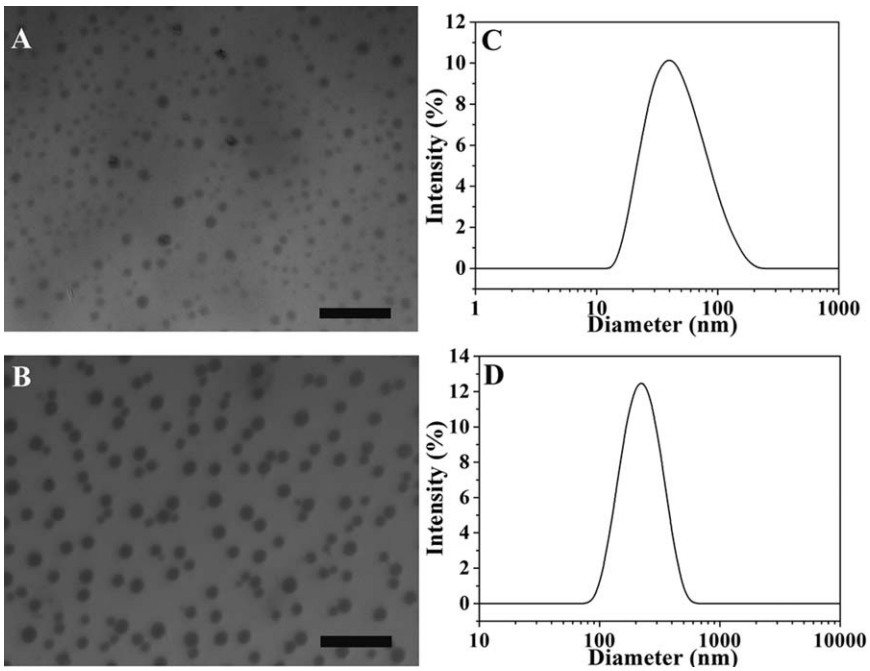

FIGURE 5 TEM images of self-assembled micellss of (A) PEG-*b*-P(OEGEEMA-*co*-AzPMA) and (B) PEG-*b*-P(OEGEEMA-*co*-AzPMA-PTX)$_3$; DLS curves of micelle aqueous solutions of (C) PEG-*b*-P(OEGEEMA-*co*-AzPMA) and (D) PEG-*b*-P(OEGEEMA-*co*-AzPMA-PTX)$_3$, scale bar = 200 nm.

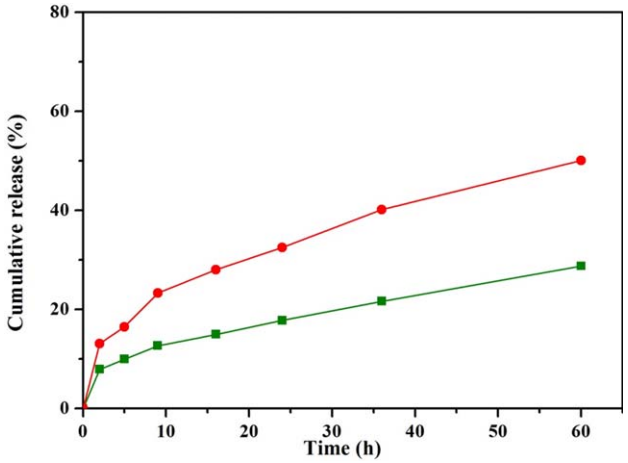

FIGURE 6 *In vitro* PTX release profiles recorded for the aqueous solution of diblock copolymer PEG-*b*-P(OEGEEMA-*co*-AzPMA-PTX)$_3$ conjugate at (■) pH 7.4 and (●) pH 5.5. [Color figure can be viewed in the online issue, which is available at wileyonlinelibrary.com.]

absorption was further used to verify the structure of PEG-*b*-P(OEGEEMA-*co*-AzPMA-PTX) as shown in Figure 4. Compared with the spectrum of PEG-*b*-P(OEGEEMA-*co*-AzPMA), each spectrum of PEG-*b*-P(OEGEEMA-*co*-AzPMA-PTX)$_s$ showed a characteristic absorption band at 229 nm, confirming the existence of PTX in the copolymer conjugate. The intenisity of the absorption peak at 229 nm increased with the PTX content. Thus, the drug loading content of PEG-*b*-P(OEGEEMA-*co*-AzPMA-PTX)$_s$ could be determined by GPC, ^{1}H NMR, and UV-Vis. The results were listed in Table 1, and the drug loading contents determined by different methods were consistent. In the following experiment, PEG-*b*-P(OEGEEMA-*co*-AzPMA-PTX)$_3$ was selected because of its high drug loading level.

The resultant PEG-*b*-P(OEGEEMA-*co*-AzPMA-PTX) conjugate was amphiphilic, and could self-assemble into micelles in aqueous solution. The hydrophobic inner core of the micelles was composed of hydrophobic PTX, whereas the outer shell was composed of hydrophilic PEG, which provided good hydrophilicity and biocompatibility. The size of the micelles is an important parameter for drug delivery. Micelles with a diameter of 50∼200 nm are beneficial to maintain a lower level of reticuloendothelial system uptake and efficient EPR effect for passive tumor targeting. The size and morphology of the self-assembled PEG-*b*-P(OEGEEMA-*co*-AzPMA-PTX) conjugate were characterized by TEM and DLS. As it was shown in the DLS results of Figure 5, both of the diblock copolymer micelles and PEG-*b*-P(OEGEEMA-*co*-AzPMA-PTX)$_3$ conjugate micelles were relatively monodisperse, exhibiting an intensity-average hydrodynamic diameter of 43 nm and 150 nm, respectively. PEG-*b*-P(OEGEEMA-*co*-AzPMA) micelles are not a single micelle, but micellar aggregates. After loading PTX, the PEG-*b*-P(OEGEEMA-*co*-AzPMA-PTX)$_3$ conjugates aggregated to larger micelles, because of their higher molecular weight and the introduction of hydrophobic PTX, which increased the hydrophobicity of the polymers. TEM images revealed that both the diblock copolymer micelles and PTX-polymer conjugate micelles were fairly monodisperse and spherical nanoparticles.

As mentioned earlier, the burst release of loaded drug is a long-standing chanllenge, and it can lead to undesirable side effects and reduce the therapeutic efficacy.[58] Typically, DDSs drug loading via noncovalent interactions often burst release 60–90% of their payloads within a few hours, because the release behavior of drug is controlled solely by diffusion.[59] In contrast, drug covalently loaded DDSs appear to be more stable, as long as the covalent linkages remain intact. As described above, PTX was covalently conjugated to PEG-*b*-P(OEGEEMA-*co*-AzPMA) by a click reaction. The ester bond of PTX-copolymer could be slowly hydrolyzed, and then PTX was released. The *in vitro* drug release profiles of PEG-*b*-P(OEGEEMA-*co*-AzPMA-PTX)$_3$ conjugate were evaluated under simulated physiological condition and mildly acidic pH. As seen from Figure 6, the amount of PTX released from PEG-*b*-P(OEGEEMA-*co*-AzPMA-PTX)$_3$ was 28.8% under simulated physiological condition within 60 h. In comparison, 50% of PTX was released from PTX-polymer conjugate within 60 h at pH 5.5. Signifant acceleration of PTX release was actuated under mildly acidic condition, because an ester bond is sensitive to acid and the hydrolysis of ester is more faster under acidic environment. The above results implied that the PTX release kinetics of PEG-*b*-P(OEGEEMA-*co*-AzPMA-PTX)$_3$ conjugate was determined not only by diffusion but also by the hydrolysis of the PTX-copolymer ester linker. The release

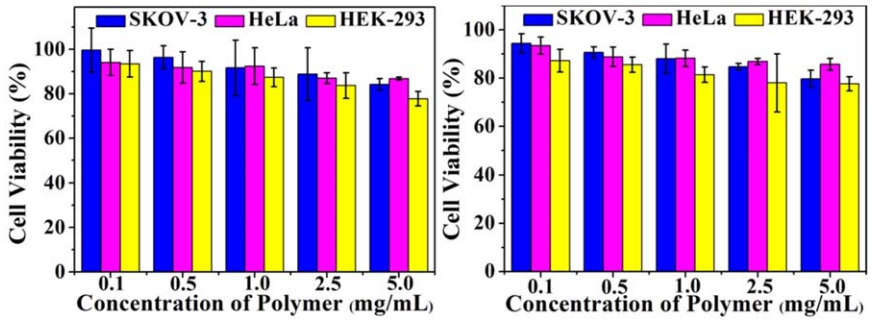

FIGURE 7 Cell cytotoxicity of PEG-*b*-P(OEGEEMA-*co*-AzPMA) against SKOV-3, Hela, and HEK-293 cells with different incubation time of (A) 24 and (B) 48 h. [Color figure can be viewed in the online issue, which is available at wileyonlinelibrary.com.]

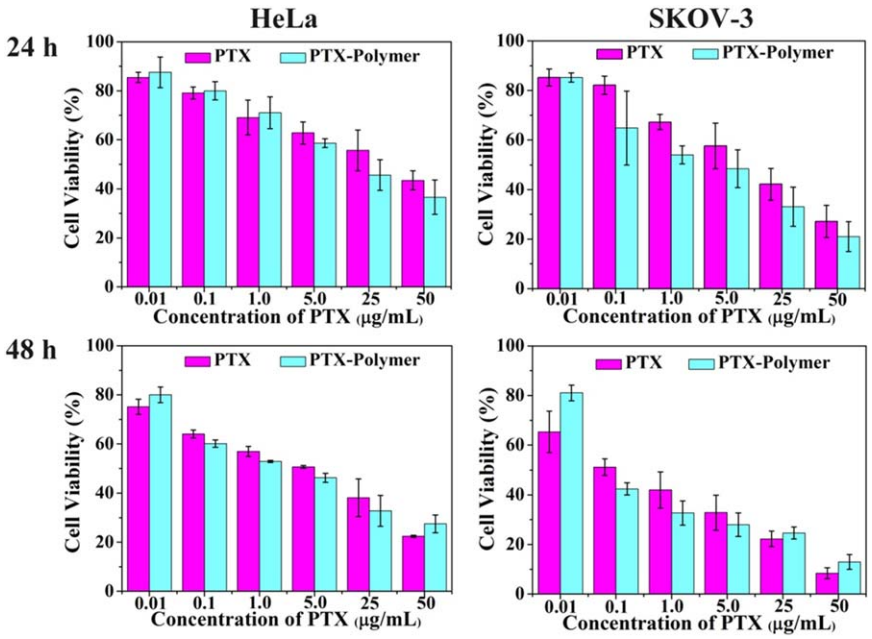

FIGURE 8 *In vitro* cell viability of Hela and SKOV-3 cells against free PTX and PEG-*b*-P(OEGEEMA-*co*-AzPMA-PTX)$_3$ at different concentrations and incubation time. [Color figure can be viewed in the online issue, which is available at wileyonlinelibrary.com.]

behavior of PTX could be controlled by varying the pH, and with a significantly reduced burst release effect.

It is very important to evaluate the potential toxicity of polymeric materials for drug delivery application. The *in vitro* cytotoxicity of PEG-*b*-P(OEGEEMA-*co*-AzPMA) against Hela, SKOV-3 (human tumor cells) and HEK-293 (human normal cells) with different concentrations and incubation times was studied by the CCK-8 assays. As seen from Figure 7, PEG-*b*-P(OEGEEMA-*co*-AzPMA) showed no obvious cytotoxic effect on Hela and SKOV-3 cells at a concentration ranged from 0.01 to 5.0 mg mL^{-1}. Even at the concentration of PEG-*b*-P(OEGEEMA-*co*-AzPMA) up to 5.0 mg mL^{-1}, the cell viability was above 80% after incubation for 48 h. Furthermore, HEK-293 cell could also tolerate the treatment with PEG-*b*-P(OEGEEMA-*co*-AzPMA) at 5.0 mg mL^{-1} for 24 h (Fig. 7). Although a slight decrease in HEK-293 cell viability was observed when the incubation time increased to 48 h, the cell viability was still nearly 75%. These results suggested the cytotoxicity of PEG-*b*-P(OEGEEMA-*co*-AzPMA) was pretty low, and suitable to use as drug carrier in DDSs.

The antitumor activity of PEG-*b*-P(OEGEEMA-*co*-AzPMA-PTX) conjugate with different drug concentrations and incubation times was studied in Hela and SKOV-3 cells using the CCK-8 assays. Free PTX was used as a control and the concentration of drug was from 0.01 to 50 μg mL^{-1}. As shown in Figure 8, after incubation for 24 h, the drug activity of polymeric micellar prodrug was better than that of free PTX in both Hela and SKOV-3 cells. This might because that PTX is a hydrophobic drug and tends to precipitate out of cell medium, leading to be difficult to enter into the cells.[32,42] However, the polymeric prodrug could self-assemble into micellar nanoparticles in aqueous solution, which were more easily internalized into the cells by cells endocytosis. Once entering into the cells, it was conceivable that the acidic pH and the enzymes in the endosomes would hydrolyze the ester bond and release PTX.[60] It was worth noting that the free drug showed more potent cellular growth inhibition abilities at high concentration with the culture time increasing to 48 h. However, the enhancements of inhibition efficiency of polymeric micellar prodrug were more obvious than that of free PTX at low concentration. This result might be related that more free PTX entered the cells at high concentration with the incubation time increasing to 48 h. The results discussed above indicated that the PEG-*b*-P(OEGEEMA-*co*-AzPMA-PTX) conjugate possessed excellent biocompatibility, high drug loading and potent antitumor effect.

CONCLUSIONS

In summary, azide-functional diblock copolymer PEG-*b*-P(OEGEEMA-*co*-AzPMA) was synthesized and alkyne-functional PTX was conjugated to this copolymer using click chemistry. The novel PTX-polymer conjugate could self-assemble into micellar nanoparticles in aqueous solution, and the loading content of PTX could be easily tuned by the feeding ratio. The chemical structures of the diblock copolymer and PTX-polymer conjugate were determined by ^{1}H NMR, GPC, FT-IR, and UV characterizations. The PEG-*b*-P(OEGEEMA-*co*-AzPMA-PTX) drug-polymer conjugate showed cumulative release of PTX at pH 7.4, and accelerated drug release at pH 5.5. *In vitro* CCK-8 assays demonstrated that PEG-*b*-P(OEGEEMA-*co*-AzPMA) exhibited low cytotoxicity, and PTX-polymer conjugate could efficiently deliver PTX into Hela and SKOV-3 cells, leading to excellent antitumor activity. The strategy of using polymers as drug carriers and PTX conjugated to polymers via click chemistry provides an important alternative for developing new drug delivery systems.

ACKNOWLEDGMENTS

The authors thank the financial support from the National Natural Science Foundation of China (51073042, 81000278, 51103026, 51373035, and 51373040), the Shanghai Natural Science Funds (11ZR1403100), the Shanghai Scientific and Technological Innovation Project (11JC1400600 and 10431903000), the Shanghai Rising Star Program (12QB1402900), the Specialized Research Fund for the Doctoral Program of Higher Education (20110071120006), School of Pharmacy, Fudan University, and The Open Project Program of Key Lab of Smart Drug Delivery (Fudan University), Ministry of Education and PLA, China.

REFERENCES AND NOTES

1 X. L. Feng, F. T. Lv, L. B. Liu, H. W. Tang, C. F. Xing, Q. O. Yang, S. Wang. *ACS Appl. Mater. Inter.* **2010**, *2*, 2429–2435.

2 Y. Li, L. Zou, Y. Li, B. Haibe-Kains, R. Y. Tian, Y. Li, C. Desmedt, C. Sotiriou, Z. Szallasi, J. D. Iglehart, A. L. Richardson, Z. C. Wang. *Nat. Med.* **2010**, *16*, 241–U121.

3 N. S. Rejinold, K. P. Chennazhi, H. Tamura, S. V. Nair, R. Jayakumar. *ACS Appl. Mater. Inter.* **2011**, *3*, 3654–3665.

4 J. Tournebize, A. Boudier, A. Sapin-Minet, P. Maincent, P. Leroy, R. Schneider. *ACS Appl. Mater. Inter.* **2012**, *4*, 5790–5799.

5 M. J. Hawkins, P. Soon-Shiong, N. Desai. *Adv. Drug Delivery Rev.* **2008**, *60*, 876–885.

6 T. Chen, S. Xu, T. Zhao, L. Zhu, D. F. Wei, Y. Y. Li, H. X. Zhang, C. Y. Zhao. *ACS Appl. Mater. Inter.* **2012**, *4*, 5766–5774.

7 M. C. Wani, H. L. Taylor, M. E. Wall, P. Coggon, A. T. McPhail. *J. Am. Chem. Soc.* **1971**, *93*, 1797–1805.

8 U. Manna, S. Patil. *ACS Appl. Mater. Inter.* **2010**, *2*, 1521–1527.

9 A. K. Singla, A. Garg, D. Aggarwal. *Int. J. Pharm.* **2002**, *235*, 179–192.

10 M. Q. Li, W. T. Song, Z. H. Tang, S. X. Lv, L. Lin, H. Sun, Q. S. Li, Y. Yang, H. Hong, X. S. Chen. *ACS Appl. Mater. Inter.* **2013**, *5*, 1781–1792.

11 J. W. J. Singer. *Control. Release* **2005**, *109*, 120–126.

12 Y. Bae, S. Fukushima, A. Harada, K. Kataoka. *Angew. Chem. Int. Ed.* **2003**, *42*, 4640–4643.

13 D. Yang, F. Yang, J. H. Hu, J. Long, C. C. Wang, D. L. Fu, Q. X. Ni. *Chem. Commun.* **2009**, *29*, 4447–4449.

14 W. A. McMaster, X. J. Wang, R. A. Caruso. *ACS Appl. Mater. Inter.* **2012**, *4*, 4717–4725.

15 F. Wang, Y. C. Wang, S. Dou, M. H. Xiong, T. M. Sun, J. Wang. *ACS Nano* **2011**, *5*, 3679–3692.

16 S. M. Lee, T. V. O'Halloran, S. T. Nguyen. *J. Am. Chem. Soc.* **2010**, *132*, 17130–17138.

17 L. Yuan, W. L. Chen, J. H. Hu, J. Z. Zhang, D. Yang. *Langmuir* **2013**, *29*, 734–743.

18 K. Niikura, N. Iyo, Y. Matsuo, H. Mitomo, K. Ijiro. *ACS Appl. Mater. Inter.* **2013**, *5*, 3900–3907.

19 B. Sahoo, K. S. P. Devi, R. Banerjee, T. K. Maiti, P. Pramanik, D. Dhara. *ACS Appl. Mater. Inter.* **2013**, *5*, 3884–3893.

20 K. Kataoka, G. S. Kwon, M. Yokoyama, T. Okano, Y. J. Sakurai. *Control. Release* **1993**, *24*, 119–132.

21 J. M. Zhu. *Biomaterials* **2010**, *31*, 4639–4656.

22 X. B. Xiong, A. Falamarzian, S. M. Garg, A. J. Lavasanifar. *Control. Release* **2011**, *155*, 248–261.

23 D. Peer, J. M. Karp, S. Hong, O. C. FaroKHzad, R. Margalit, R. Langer. *Nat. Nanotechnol.* **2007**, *2*, 751–760.

24 M. E. Fox, F. C. Szoka, J. M. Frechet. J. Acc. *Chem. Res.* **2009**, *42*, 1141–1151.

25 K. Kataoka, T. Matsumoto, M. Yokoyama, T. Okano, Y. Sakurai, S. Fukushima, K. Okamoto, G. S. J. Kwon. *J. Control. Release* **2000**, *64*, 143–153.

26 N. Rapoport. *Prog. Polym. Sci.* **2007**, *32*, 962–990.

27 E. R. Gillies, J. M. J. Frechet. *Chem. Commun.* **2003**, *14*, 1640–1641.

28 J. Yao, Y. L. Ruan, T. Zhai, J. Guan, G. P. Tang, H. R. Li, S. Dai. *Polymer* **2012**, *52*, 3396–3404.

29 N. Bailly, M. Thomas, B. Klumperman. *Biomacromolecules* **2012**, *13*, 4109–4117.

30 M. Q. Li, Z. H. Tang, H. Sun, J. X. Ding, W. T. Song, X. S. Chen. *Polym. Chem.* **2013**, *4*, 1199–1207.

31 S. C. Lee, K. M. Huh, J. Lee, Y. W. Cho, R. E. Galinsky, K. Park. *Biomacromolecules* **2007**, *8*, 202–208.

32 X. J. Li, Y. F. Qian, T. Liu, X. L. Hu, G. Y. Zhang, Y. Z. You, S. Y. Liu. *Biomaterials* **2011**, *32*, 6595–6605.

33 Y. Bae, K. Kataoka. *Adv. Drug Delivery Rev.* **2009**, *61*, 768–784.

34 K. J. Pekarek, J. S. Jacob, E. Mathiowitz. *Nature* **1994**, *367*, 258–260.

35 V. Torchilin. *Adv. Drug Delivery Rev.* **2011**, *63*, 131–135.

36 L. M. Kaminskas, V. M. McLeod, C. J. H. Porter, B. J. Boyd, *Mol. Pharmaceutics* **2012**, *9*, 355–373.

37 X. P. Ma, Q. H. Sun, Z. X. Zhou, E. L. Jin, J. B. Tang, E. V. Kirk, W. J. Murdoch, Y. Q. Shen. *Polym. Chem.* **2013**, *4*, 812–819.

38 Y. Bae, N. Nishiyama, K. Kataoka. *Bioconjugate Chem.* **2007**, *18*, 1131–1139.

39 A. Ponta, Y. Bae. *Pharm. Res.* **2010**, *27*, 2330–2342.

40 C. Clementi, K. Miller, A. Mero, R. Satchi-Fainaro, G. Pasut. *Mol. Pharmaceutics* **2011**, *8*, 1063–1072.

41 F. Greco, I. Arif, R. Botting, C. Fante, L. Quintieri, C. Clementi, O. Schiavon, *G. Pasut. Polym. Chem.* **2013**, *4*, 1600–1609.

42 A. W. Alani, Y. Bae, D. A. Rao, G. S. Kwon. *Biomaterials* **2010**, *31*, 1765–1772.

43 A. K. Patri, J. F. Kukowska-Latallo, J. R. Baker. *Adv. Drug Delivery Rev.* **2005**, *57*, 2203–2214.

44 P. L. Golas, K. Matyjaszewski. *Chem. Soc. Rev.* **2010**, *39*, 1338-1354.

45 Y. Yu, J. Zou, L. Yu, W. Ji, Y. K. Li, W. C. Law, C. Cheng. *Macromolecules* **2011**, *44*, 4793–4800.

46 J. Han, D. D. Zhu, C. Gao. *Polym. Chem.* **2013**, *4*, 542–549.

47 M. Talelli, K. Morita, C. J. F. Rijcken, R. W. M. Aben, T. Lammers, H. W. Scheeren, C. F. van Nostrum, G. Storm, W. E. Hennink. *Bioconjugate Chem.* **2011**, *22*, 2519–2530.

48 L. Yuan, W. L. Chen, J. Li, J. H. Hu, J. J. Yan, D. J. Yang. *J. Polym. Sci. Part A: Polym. Chem.* **2012**, *50*, 4579–4588.

49 L. Tong, S. Zhong, Z. Sen, Y. J. Li, G. L. Lu, X. Y. Huang. *Polymer* **2008**, *49*, 4534–4540.

50 L. Tong, S. Zhong, D. Yang, S. Chen, Y. J. Li, J. H. Hu, G. L. Lu, X. Y. Huang. *Polymer* **2009**, *50*, 2341–2348.

51 B. S. Sumerlin, N. V. Tsarevsky, G. Louche, R. Y. Lee, K. Matyjaszewski. *Macromolecules* **2005**, *38*, 7540–7545.

52 S. J. Zhai, J. Shang, D. Yang, S. Y. Wang, J. H. Hu, G. L. Lu, X. Y. J. Huang. *J. Polym. Sci. Part A: Polym. Chem.* **2012**, *50*, 811–820.

53 X. M. Song, Y. Q. Zhang, D. Yang, L. Yuan, J. H. Hu, G. L. Lu, X. Y. Huang. *J. Polym. Sci. Part A: Polym. Chem*. **2011**, *49*, 3328–3337.

54 Q. Zhang, Z. Shen, D. Yang, C. Feng, J. H. Hu, G. L. Lu, X. Y. Huang. *Macromolecules* **2010**, *43*, 117–125.

55 L. N. Gu, C. Feng, D. Yang, Y. G. Li, J. H. Hu, G. L. Lu, X. Y. Huang. *J. Polym. Sci. Part A: Polym. Chem*. **2009**, *47*, 3142–3153.

56 C. Feng, Y. J. Li, D. Yang, J. H. Hu, X. H. Zhang, X. Y. Huang. *Chem. Soc. Rev*. **2011**, *40*, 1282–1295.

57 L. N. Gu, Z. Shen, C. Feng, Y. G. Li, G. L. Lu, X. Y. Huang. *J. Polym. Sci. Part A: Polym. Chem*. **2008**, *46*, 4056–4069.

58 X. L. Hu, H. Li, S. Z. Luo, T. Liu, Y. Y. Jiang, S. Y. Liu. *Polym. Chem*. **2013**, *4*, 695–706.

59 R. Tong, J. J. Cheng. *Angew. Chem. Int. Ed*. **2008**, *47*, 4830–4834.

60 G. L. Li, J. Y. Liu, Y. Pang, R. B. Wang, L. M. Mao, D. Y. Yan, X. Y. Zhu. *Biomacromolecules* **2011**, *12*, 2016–2026.